Journal of Alloys and Compounds 637 (2015) 382–392

Contents lists available at ScienceDirect

Journal of Alloys and Compounds

journal homepage: www.elsevier.com/locate/jalcom

Development of smart oxidation and corrosion resistance of multi-doped complex hybrid coatings on mild steel

O.S.I. Fayomi [a,b,*], A.P.I. Popoola [a]

[a] Department of Chemical, Metallurgical and Materials Engineering, Tshwane University of Technology, P.M.B. X680, Pretoria, South Africa
[b] Department of Mechanical Engineering, Covenant University, P.M.B 1023, Ota, Ogun State, Nigeria

ARTICLE INFO

Article history:
Received 22 January 2015
Received in revised form 18 February 2015
Accepted 20 February 2015
Available online 28 February 2015

Keywords:
$Zn–Al–SnO_2–TiO_2$
Composite
Multifunctional deposition
Interfacial interaction

ABSTRACT

The microstructure, mechanical and thermal treatment behavior of $Zn–Al–SnO_2/TiO_2$ (Zn–Al–Sn/Ti) produced through chloride deposition system was studied. 7.0–13.0 wt% TiO_2 and SnO_2 was added to chloride Zn–Al bath. A thermal treatment characteristic was done for 2 h at 200 °C, 400 °C and 600 °C. The ageing behaviors of the co-deposited alloys were evaluated using (SEM/EDS) and XRD. The hardness and wear value of the solid coatings were examined with micro-hardness and UMT-2 sliding tester respectively. The corrosion properties were investigated by linear polarization method in 3.65% NaCl environment. From the obtained results, the deposited alloys revealed excellent stability. The even distribution of the particulate on the produced coating and thermal-treatment were observed to cause the improvement on mechanical, tribological and electrochemical properties. The overall best coating was obtained at Zn–Al–7Sn–Ti–0.3V–Cl for as-coated and Zn–Al–7Sn–Ti–0.3V–Cl at 400 °C for the thermo-mechanical treated samples. The hardness, corrosion and micro-mechanical resistance performance against the working substrate were depended on the development of coherent and regular precipitation from the incorporated strengthening particulate.

1. Introduction

Despite the impact of zinc based coatings as a result of their excellent mechanical and electrochemical resistance properties for steel protection in industrial applications, their less becoming popular are due to poor reaction in atmospheric environment and lesser life-span from thermal and mechanical fallout [1–4]. Consequently, tremendous approaches from literature survey to improve on this limitation are being made on the use of metal–reinforcement composite combination and manufacturing process variables [5–13]. Lately the intention on the choice of composite particulate is due to their significant constituent of solid grains and the novel attention such properties gives in advanced materials [1,14–20].

The suspended co-deposition of metal composite such as SiO_2 [16,22], Cr_2O_3, TiO_2 [19,20], ZrO_2, Al_2O_3 SnO_2 CeO_2 and ZnO [19–25] had been established to offer vital functional individual properties. However [1] attested that for excellent application especially in high temperature performance, high surface modifications are required and incorporation of high temperature composite particle had been proven to provide such safeguard. Regrettably, results on modified-binary composite alloys through this route are prone to possess possible limitation for high temperature performance, wear vulnerability and electrochemical defects.

Furthermore the control of formulated variable for advance materials also has been crucial consideration in metal matrix composite co-deposition. The wear deformation characteristics, corrosion resistance, thermo-mechanical stability and tribo-oxidation behavior of binary alloy composite coating have been reported to give stability only at ambient environment [1,21]. To the best of our knowledge from literature, there were no works done on quaternary particle reinforced using electrolytic route on Al, TiO_2 and SnO_2 especially when subjected to the heat-treatment and wear behavior for multi-facial application in single system. Although, there individual characteristics are known for exceptional properties on zinc blend [18,19,23,26].

In the light of this, since bath formulation and process parameter constitute to the kind of coating properties. We have attempted a successful sulphates produced quaternary alloy in our previous work [1] in a view to improve the tribological and poor thermal stability of the binary-modified composite coating. Our aim in this study is to fabricate a chloride modified structure by quaternary

* Corresponding author at: Department of Chemical, Metallurgical and Materials Engineering, Tshwane University of Technology, P.M.B. X680, Pretoria, South Africa. Tel.: +27 719811277.
E-mail address: ojosundayfayomi3@gmail.com (O.S.I. Fayomi).

http://dx.doi.org/10.1016/j.jallcom.2015.02.154
0925-8388/

metal composite matrix which will offer good thermal stability; improve micro-mechanical properties, and excellent corrosion behavior with stable interfacial characteristics. The wear and structural properties of the co-deposited alloy was evaluated using sliding wear tester, and their morphological crystal structure/topography was characterized by means [AFM, SEM/EDS and OPM]. The phase patterns were examined with the help of X-ray diffractometer (XRD) and Raman.

2. Experimental procedure

2.1. Preparation of substrates

Sectioned flat specimens from commercially sourced mild steel of (40 mm × 20 mm × 1 mm) sheet was used as cathode substrate and 99.5% zinc plate of (30 mm × 20 mm × 1 mm) were prepared as anodes. The initial surface preparation was performed with finer grade of emery paper as described in our previous studies [1,9]. The sample were properly cleaned with sodium carbonate, pickled and activated with 10% HCl at ambient temperature for 10 s then followed by instant rinsing in deionized water. The mild steel specimens were obtained from metal sample site in Nigeria. The chemical composition of the sectioned samples is shown in Table 1 as obtained from spectrometer analyzer.

2.2. Processed composition

The electrolytic chemical bath of Zn–Al–Sn–Ti fabricated alloy was performed in a single cell containing two zinc anode and single cathode electrodes as described schematically as reported by [1]. The distance between the anode and the cathode is 15 mm. Before the plating, all chemical used are analar grade and de-ionized water were used in all solution admixed. The bath was preheated at 40 °C. The processed parameter and bath composition admixed used for the different coating matrix is as follows Zn 75 g/L, Al 30 g/L, KCl 50 g/L, ZnCl 75 g/L, Boric acid 10 g/L, SnO_2 7 g–13 g/L, TiO_2 7 g–13 g/L, pH 4.8, time, 20 min and tempt 40 °C. The choice of the deposition parameter is in line with the preliminary study from our previous work [1] (see Table 2).

The prepared zinc electrodes were connected to the rectifier at varying applied potential and current density between 0.3 V and 0.5 V at 2 A/cm^2 for 20 min. The distance between the anode and the cathode with the immersion depth were kept constant as described by Fayomi et al. [18]. The fabricated alloys were rinsed in distilled water and samples air-dried. Portion of the coating were sectioned for characterization.

2.3. Characterization of coating

The structural evolution of the deposited composite coating alloy was characterized with VEGA TESCAN scanning electron microscope equipped with EDS. The phase change was verified with XRD. Micro-hardness studies were carried out using a diamond pyramid indenter EMCO Test Dura-scan micro-hardness testers at a load of 10 g for a period of 20 s. The average microhardness trend was measured across the coating interface in an interval of 2 cm using screw gauge attached to the Dura hardness tester.

2.4. Friction and wear tests

The friction and wear properties of the deposited quaternary fabricated alloy were measured using CERT UMT-2 tribological tester at ambient temperature of 25 °C with schematic diagram as reported by [1]. The reciprocating sliding tests was carried out with a load of 5 N, constant speed of 5 mm/s, displacement amplitude of 2 mm in 20 min. A Si_3N_4 ball (4 mm in diameter, HV50g1600) was chosen as counter body for the evaluation of tribological behavior of the coated sample. The dimension of the wear specimen is 2 cm by 1.5 cm as prescribed by the specimen holder. After the wear test, the structure of the wear scar and film worn tracks are further examined with the help of high Nikon Optical Microscope (OPM) and scanning electron microscope couple with energy dispersive spectroscopy (VEGAS-TESCAN SEM/EDS).

Table 1
Spectrometer chemical composition of mild steel used (wt%).

Element	C	Mn	Si	P	S	Al	Ni	Fe
Composition	0.15	0.45	0.18	0.01	0.031	0.005	0.008	99.166

Table 2
Itinerary bath composition of quaternary Zn–Al–Sn–Ti–Cl alloy co-deposition.

Sample order	Material sample	Time of deposition (min)	Potential (V)	Current density (A/cm^2)	Con. of additive (g)
Blank	–	–	–	–	–
Sample 1	Zn–Al–7Sn–Ti–0.3V–Cl	20	0.3	2 A	7
Sample 2	Zn–Al–7Sn–Ti–0.5V–Cl	20	0.5	2 A	7
Sample 3	Zn–Al–13Sn–Ti–0.3V–Cl	20	0.3	2 A	13
Sample 4	Zn–Al–13Sn–Ti–0.5V–Cl	20	0.5	2 A	13

2.5. Thermo/electro-oxidation test

Isothermal heat treatment (direct fired furnace atmosphere) of Zn–Al–Sn–Ti composite coating was carried out between 200 and 600 °C for 1hr to enhance the mechanical stability of the coated samples. The electrochemical studies were performed with Autolab PGSTAT 101 Metrohm potentiostat using a three-electrode cell assembly in a 3.65% NaCl static solution at 40 °C. The developed composite was the working electrode, platinum electrode was used as counter electrode and Ag/AgCl was used as reference electrode. The anodic and cathodic polarization curves were recorded by a constant scan rate of 0.012 V/s which was fixed from ±1.5 mV. From the Tafel corrosion analysis, the corrosion rate, potential and linear polarization resistance was obtained.

3. Results and discussion

3.1. Structural characterization

SEM/EDS of the as-received mild steel substrate are presented in Fig. 1. The microstructure of the electro-fabricated Zn–Al–Sn–Ti alloy composite matrix additions are shown in Fig. 2. The deposits with 7 wt% in 0.3 V revealed a reasonable uniform distribution and a small micro particle inter-link around the major metal lattice. The coating exhibits a new morphology with adorable structural grain. The produced deposits show interference of SnO_2 and TiO_2 evenly conditioned into the Zn–Al–Sn–Ti matrix. The EDS quantification identifies the major embedded particles. A visible coverage by composite micro-crystallites without crack was seen. The structure yield good quality deposit which is attributed to the miscible and excellent control of process parameter of the bath which is in line with the report by Chuen-Chang and Chi-Ming [3]

The activities surrounding the nature of the distributed microstructure can be link to alumina–tin–titanium particles migration assisted by slow/lower potential of deposition. In general solid interfacial precipitation occurs between the integrated particles and the based zinc rich. Secondly, the morphologies obtained which show a well dispersed crystal might also be traced to the influence of additive admixed in the bath and agitation of the bath to disallow agglomeration thereby preventing the initiation of stress propagation [20,21]. Although Rahman et al. [11] said in co-deposition process, crystallization influence the structure and its properties, crystallization exist either by buildup of old crystals or by formation and growth of new one through the deposition rate thereby causing nucleation within the cathode surface and further help to enhance preferential sites.

Comparing these micrographs, with alloy produced at 13 wt% induced at 0.3 V there seems to be de-agglomeration like the formal. However, the movement of particles toward the cathode region could have cause the embedded solid particle within the interface to be stress and in so doing given rise to few crack and pores seen at the interface (see Fig. 2b). According to [19] the nature of composite coating produced can be influenced by the absorption of incorporation and control of process parameter. Hence, increase power or potential, increases further the

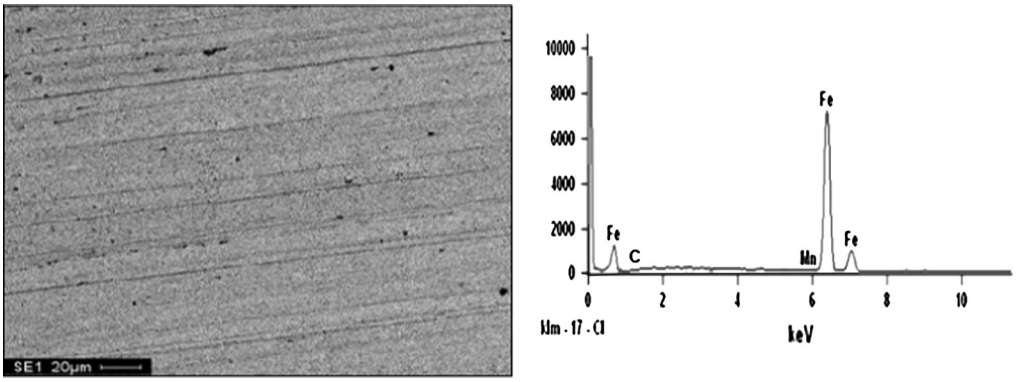

Fig. 1. SEM/EDS of mild steel substrate.

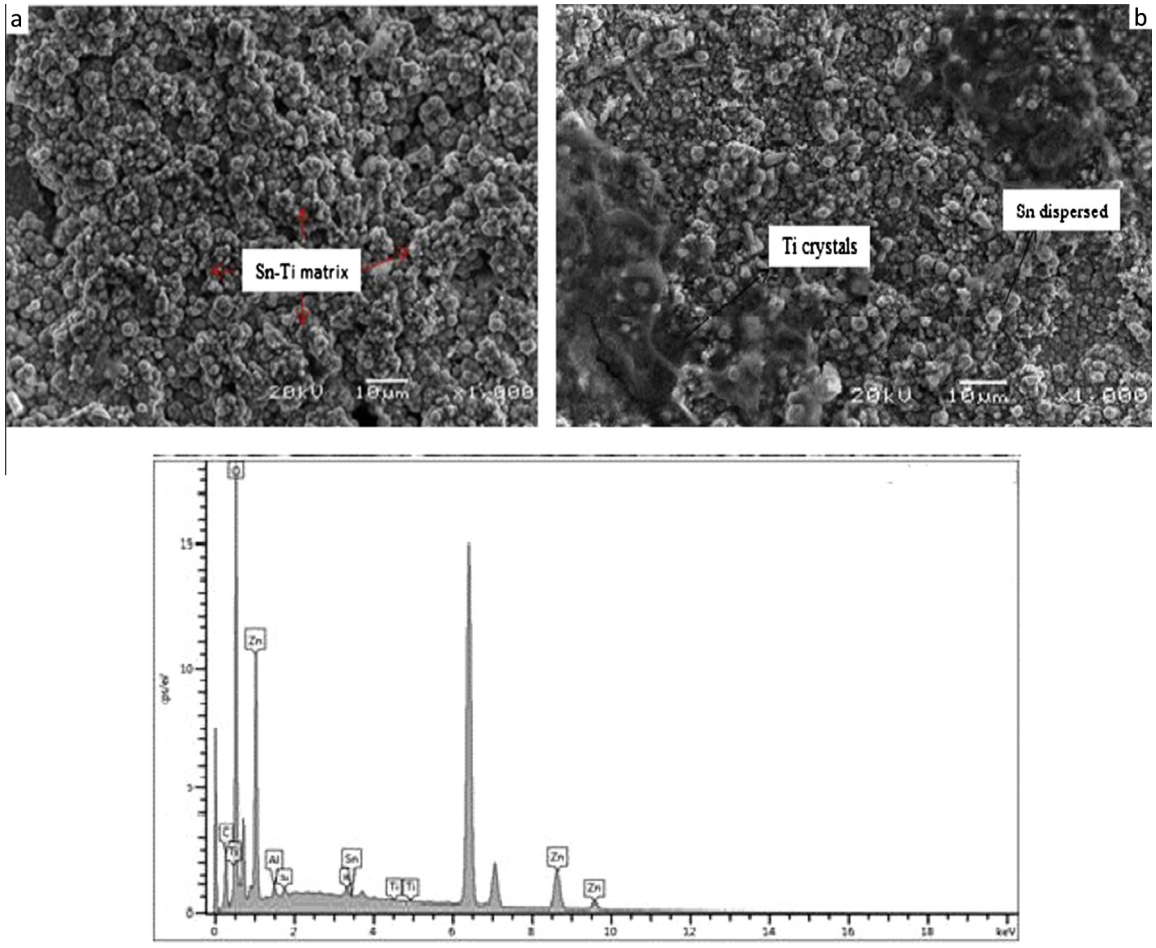

Fig. 2. Micrograph showing the surface morphology of (a) SEM of Zn–Al–7Sn–Ti–0.3V and (b) SEM/EDX of Zn–Al–13Sn–Ti–0.3V chloride composite coating.

embedment of particulate on steel substrate. This assessment poses appearance of pores at deposited interface which is in line with our observation in result reported in Fig. 2b.

3.2. Atomic force microstructural studies

Fig. 3a and b shows atomic force image of co-deposited structures at different condition. For the sample with Zn–Al–7Sn–Ti–0.3V concentrations in bath control of 7 wt%, the topography and distribution of the deposited alloy are stable all through the interface. From all indications, grain size and crystal growth uniformity was obtained within Fig. 3a matrix. The distribution of the composite topography within the metal matrix was not even when increased to 13 wt%. It is evidence that within the frame dispatched of 7 wt% good refinements in grain size and better microstructural modification were obtained from the general topographic image. The vast buildup of the crystallites are attributed to the deposition rate which was in agreement with the statement made from the study by [13] that increasing the concentrations of composite might propagate and lead to the increase in the deposition rate, hence making nucleation process precede the crystallites growing rate. Another important observation is that grains

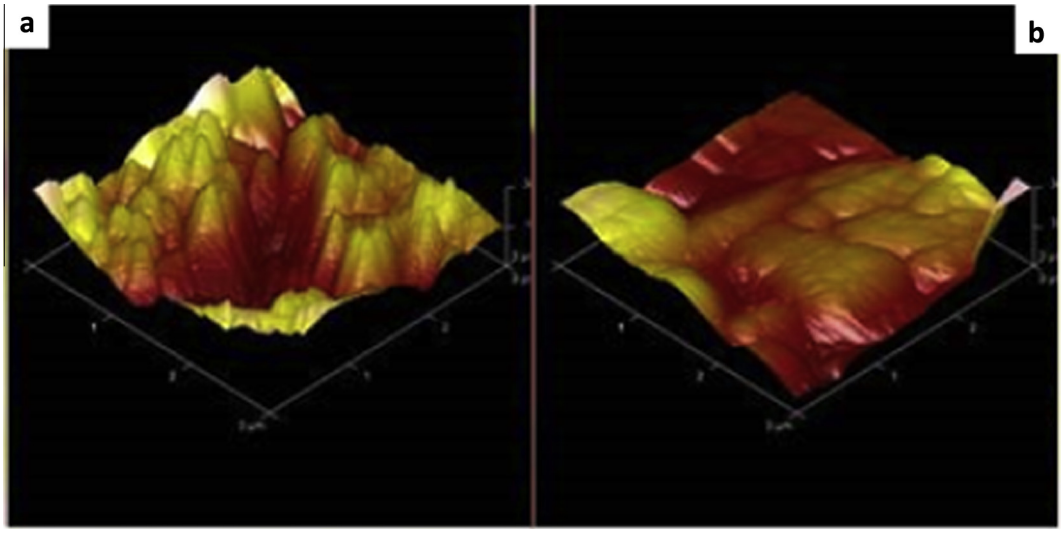

Fig. 3. AFM of (a) Zn–Al–7Sn–Ti–Cl–0.3V alloy and (b) Zn–Al–13Sn–Ti–Cl–0.3V alloy.

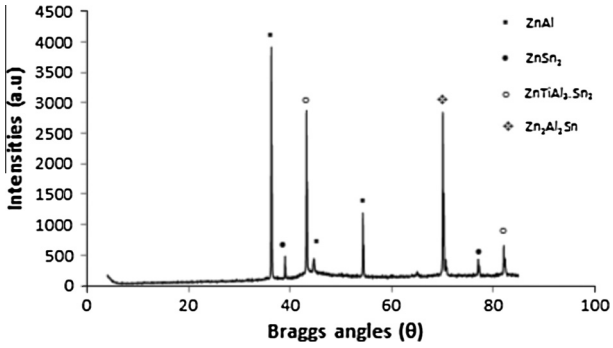

Fig. 4. X-ray diffraction pattern for Zn–Al–7Sn–Ti–0.3V.

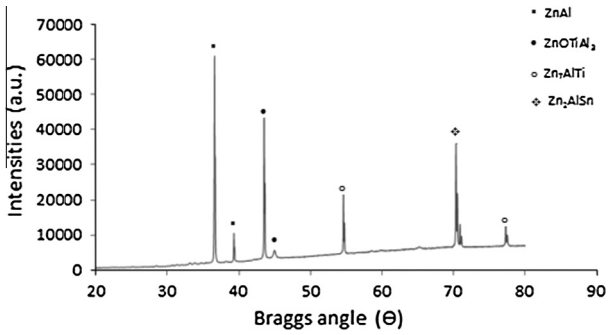

Fig. 5. X-ray diffraction pattern for Zn–Al–13Sn–Ti–0.3V.

were smaller and adherent properties were achieved with incorporated particles of 7 wt%. This is attributed to the proper diffusion of the particle into the nucleus.

An established report by [11,26] attested that it is possible for larger number of tiny composite metal be found on the working substrate without necessarily providing a nucleation site. Hence, from our observation, porous free nature and topography of 7 wt% particulate are due to smaller grain size of the coating fabricated at smaller current density and potential. According to [7] the grain size increases with the film thickness. The high rich in Zn–Al–7Sn–Ti–0.3V chloride gave a homogeneous distribution; crack free with fewer pores.

3.3. XRD/Raman studies

The XRD patterns of the thin film made from Zn–Al–7Sn–Ti–Cl–0.3V composite coating are presented in Figs. 4 and 5. The presence of the intermediate dispatched composite phases observed was traceable to ion of each particulate as described by [14,27]. Meanwhile, modification and new orientation of the metal matrix are indication of the harness performance and remarkable effect of the composite induced. ZnAl, $ZnSn_2$, $ZnTiAl_3{\cdot}Sn_2$ and Zn_2Al_2Sn were identified in the coating intermediate for Zn–Al–7Sn–Ti–Cl–0.3V fabricated coating. Although, the result inferred that Sn content had satisfactory phase above the Ti in their intermetallic patterns. It is a clear understanding when considering the phases in deposits that the height of any peak is considered as an indication of the quantity of its phase in the deposit [11]. Hence, an observed multi-phase of $ZnTiAl_3{\cdot}Sn_2$ could possibly enhance the properties of the Zn–Al–7Sn–Ti–Cl–0.3V. The substantial presence of aluminum and titanium could consequently promote an improvement in properties such as hardness and corrosion resistance.

More so, it is of necessity to say that Al, Ti and Sn peak does not observed to exist as single phase indicating that the particulate reacted homogeneously to form perfect phase presented. For the Zn–Al–13Sn–Ti–0.3V, Zn at the interfacial surface of the deposit as a single peak could be ascribed to abundance of zinc within the electrolyte. The main peaks are Zn, Zn_2AlSn, Zn_7AlTi, $ZnOTiAl_3$ phases which exist majorly at $2\theta = (38.12°, 43.10°$ and $70.22°)$. Through this phases, evidence of substantial dissolution of the composite particulate were notice to exist but not as complete as the formal with distribution at the interface.

In Fig. 6 the Raman spectrum plot of Zn–Al–7Sn–Ti chloride composite deposited layer also show a good intensity of about 1210 aμ, 210 aμ, and 210 aμ, at about 1132 cm^{-1}, 2120 cm^{-1}, and 2183 cm^{-1} respectively. This pattern shows a hexagonal or orthorhombic structure with presence of $ZnTiAl_3{\cdot}Sn_2$ buildup. The phase transformations exist significantly with Zn–Al–7Sn–Ti–0.3V within 1132–2183 cm^{-1}.

3.4. Microhardness properties

For quality check, the average micro-hardness result for Zn–Al–Sn–Ti–Cl deposition is described in Fig. 7 at varying optimized additive and voltage. The hardness profile data for all the samples

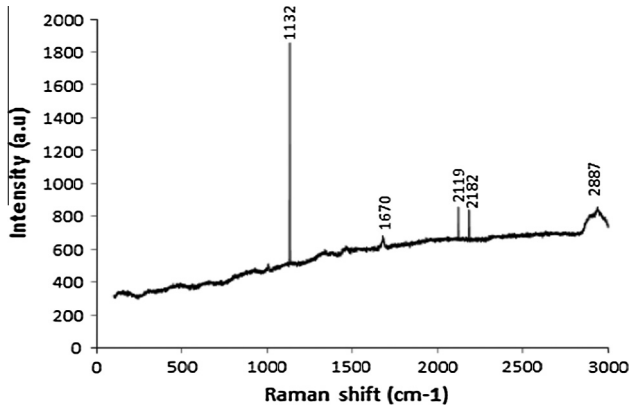

Fig. 6. Raman profile for Zn–Al–7Sn–Ti–0.3V.

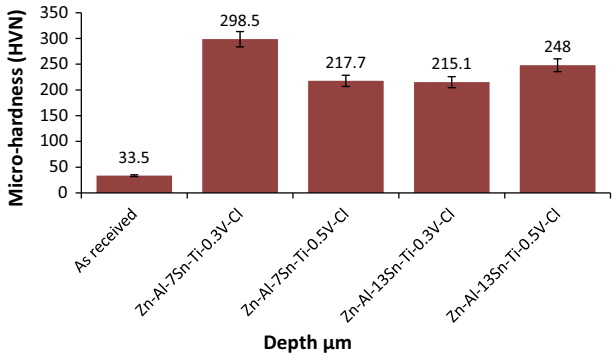

Fig. 7. The microhardness/depth profile for Zn–Al–Sn–Ti deposited sample.

show significant average increase above the as-received sample geometrically. Although, operating condition is a major factor for enhance structural properties which could also facilitate improved hardness characteristics [23,29]. Hence, microstructural evolved in coating depends on the processing parameters which are principal to the buildup of crystal [18]. From the composite coated matrix Zn–Al–7Sn–Ti–Cl–0.3V an average hardness improvement of about 298 HVN was obtained. The least among the optimized alloy coating is 215 HVN. Reason for maintaining this great edge of improved micro-hardness might not be really ascertain however, from understanding in electrodeposition processing firstly, the deposition rate at lower potential could give rise to better adhesion due to moderate throwing power. Secondly, the behavior of the conditioning particle in the process bath differs in strengthening coating. Hence, chloride bath could favor lower particles reinforcement at lower deposition rate to give a good precipitation at the cathode surface to yield the result seen.

The average microhardness (HVN) values from hardness progression shows as-received (Control) sample possessed 33.5 HVN. Next to the best produced alloy in the series after Zn–Al–7Sn–Ti–0.3V is Zn–Al–13Sn–Ti–0.5V with 248 HVN. From all facts, the improvements in hardness obviously provide a geometric increase over the substrate and this was attributed to the crystal formation and superior nucleation. The adhesion and nucleation which yield the significant micro-hardness are reported to depend on the operating condition. The combined effort of aluminum titanium and tin was noticed on the zinc matrix to accelerate the strengthening propagation of the composite fabricated coatings. In fact, report by [15] re-affirmed that blending the best properties of two or more different materials to obtain one materials having both desire properties is the major idea of composite coating

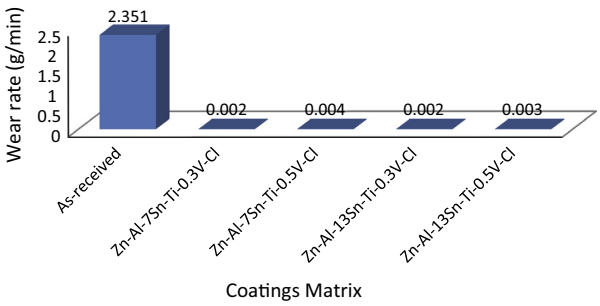

Fig. 8. Variation of the wear rate with time of Zn–Al–Sn–Ti–Cl alloy.

progress. Hence the produced improved hardness obtained is an affirmation to this result.

Consequently, unfortunately there are gradual decline in hardness behavior at higher particle incorporation. The decrease in the hardness progress as a results of over-loading of electrolyte in these series was not expected reason been that [29] attributed that increase in particle loading in the bath may result in amount of particle co-deposited on the substrate. [16] Also affirmed that hardness of the coatings is relative to the content of particles in the coatings. In this study, the proportion of particle in the embedded electrolyte and the induced power rate simultaneously influence the kind of fabricated coating seen. Above 13 g wt% there might be poor dispersion of particle which could embrace stress and obvious pores in the interface as result produce low hardness properties.

3.5. Wear rate evaluation

Fig. 8 shows variation of the wear rate as a function of time across the coating system and their deposited matrix. A remarkable improvement was obtained for all coated system as a result of improved crystal and structural modification as against the control sample. The wear loss is very high for the as-received sample with approximately 2.351 g/min; this is indeed expected. Obviously the condition for improved wear resistance was seen as a result of content of individual proportion of the metal solid grain [28]. Reported that composite coating is related to photo structure and chemical composition. Composite-SnO_2–TiO_2 hence can provide refinement in grain structure that assist in resistance to dislocation trend of the interfacial matrix at the coating interface. It is evident that Al/SnO_2/TiO_2 strengthening phase lead to the remarkable increase in anti-wear resistance as against the as-received sample. Among the produced composite coating samples Zn–Al–7Sn–Ti–0.3V–Cl and Zn–Al–13Sn–Ti–0.5V–Cl had the highest wear resistance properties. It can be said that the functional activities of multi-grains particulate enhance the change in microstructural of the coating which help to retard the progression of dislocation that may arise.

[22,30] said diffusion process of the particulate into the lattice site of base metal is a function of the weight fraction of the composite-particle in relation to the ionic migration [5]. Attested that solid particles promote wear resistance. Therefore, the positive increases in wear resistance are due to the beneficial effect of incorporated metal particle.

Figs. 9 and 10 show the variation of friction coefficients with sliding time and velocity of the deposited Zn–Al–7Sn–Ti–0.3V alloy. It is essential to mention first, that process operating in sliding wear condition such as load, sliding speed and temperature has little or no effect on frictional characteristics [6,27]. However, incorporation of the composite particulate in the zinc rich led to the decrease in friction coefficient. Although, report

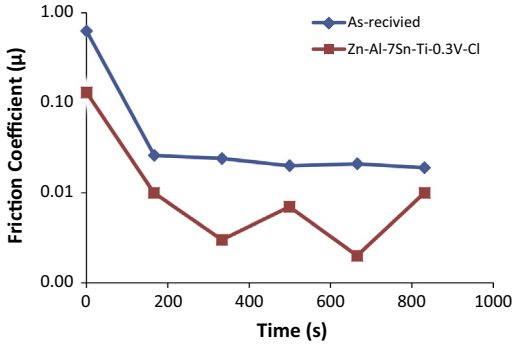

Fig. 9. Variation of wear friction co-efficient against time for Zn–Al–7Sn–0.3V chloride deposited sample.

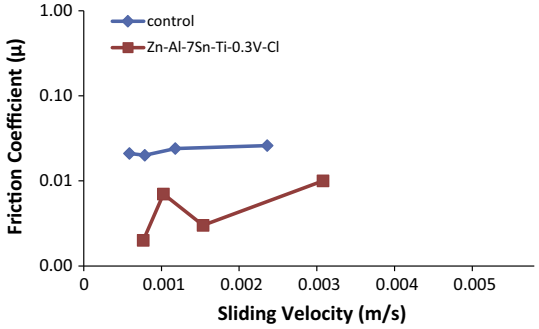

Fig. 10. Variation of wear friction co-efficient against sliding velocity for Zn–Al–7Sn–Ti–0.3V chloride deposited sample.

has shown that friction coefficient and linear wear were substantially reduced by micro-structurally modified ceramics and composite compared with monolithic alumina. The presence of admixed metal grain and composite embedded in the zinc trend has been major contribution in this studies for the advanced better friction attained as against the massive mild transition and finding reported by [24] on tribological properties for ordinary alumina based coating. In general, metal-composite-matrix interaction has been seen as a contributor for frictional resistance trend and reduced plastic deformation as observed in Figs. 9 and 10.

Figs. 11–13 show the worn scar surfaces observed after selected wear process parameter.

It can be seen from the scars, that severe degree of plastic deformation, massive grooves, and pits dominated the surface of the as-received substrate. On the other hand, for the coated materials solid grain embedded were still visibly seen along the wear track interface.

With less pit formation and unseen stress within the interface of the mild steel coatings layer, the strong adhesions of the processed fabricated coating that resist dislocation are justified by the induced film particulate. More so, the EDX studies of the wear scar shown in Fig. 12 indicated a possible elemental feature of the coating still exist within the surfaces, an evidence of strong adhesion and solid intermediate. To further compare the wear structure and the degree of damage between the Zn–Al–7Sn–Ti–0.3V and Zn–Al–13Sn–Ti–0.5V from reciprocating sliding tester results, Fig. 13a and b shows the OPM photomicrographs at the level of deformation with lower magnification.

Zn–Al–13Sn–Ti–0.5V has little debris around the edges while the formal refuse dislocation and hence pose rejection of debris along the wear track scars.

It is worth noting that composite matrix is anti-oxidative and abrasive in properties which provide resistance to certain deformation. Certain quantity of titanium oxide (TiO_2) alumina (Al_2O_3) are been found to prolong coating life span against wear and thermal influence [24,27] which is in line with our findings. More so, the anti-wear propagation of the deposited alloy was due to the interference of the composite matrix and the pool of intermetallic phase formed. The bonding characteristics and morphology were seen to justify the resilient effort to wear resistance properties observed.

3.6. Electrochemical test result

Fig. 14 shows the progression of deterioration and the susceptibility to corrode in 3.65% simulated medium with an induced current propagation examined using potential/current measurements. The differences in the potential values of the deposition were considered at 10 MA applied current. Obvious improvement in potential values was discovered as been significant which is due to the effects of coating film precipitated at the interface of the substrate. However, the substrate have less passive film formed on its surface resulting into intensive corrosion attack from the chloride solution with potential value of about −1.5 V which is

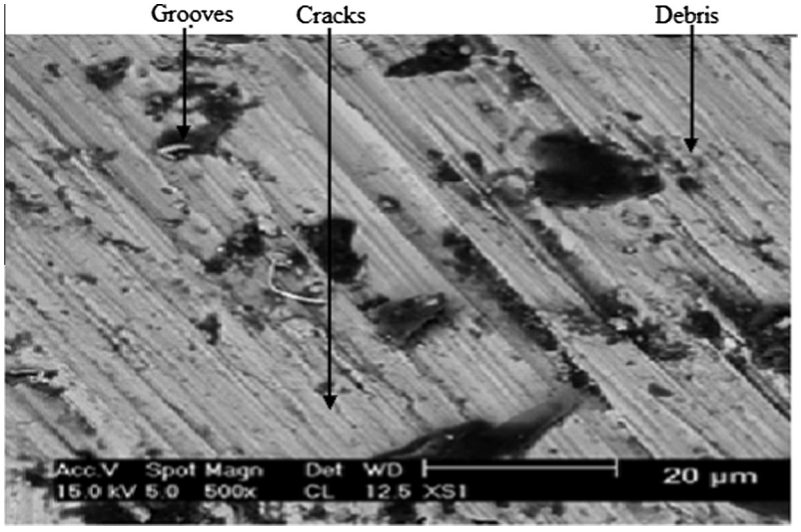

Fig. 11. SEM image of the wear scar of mild steel.

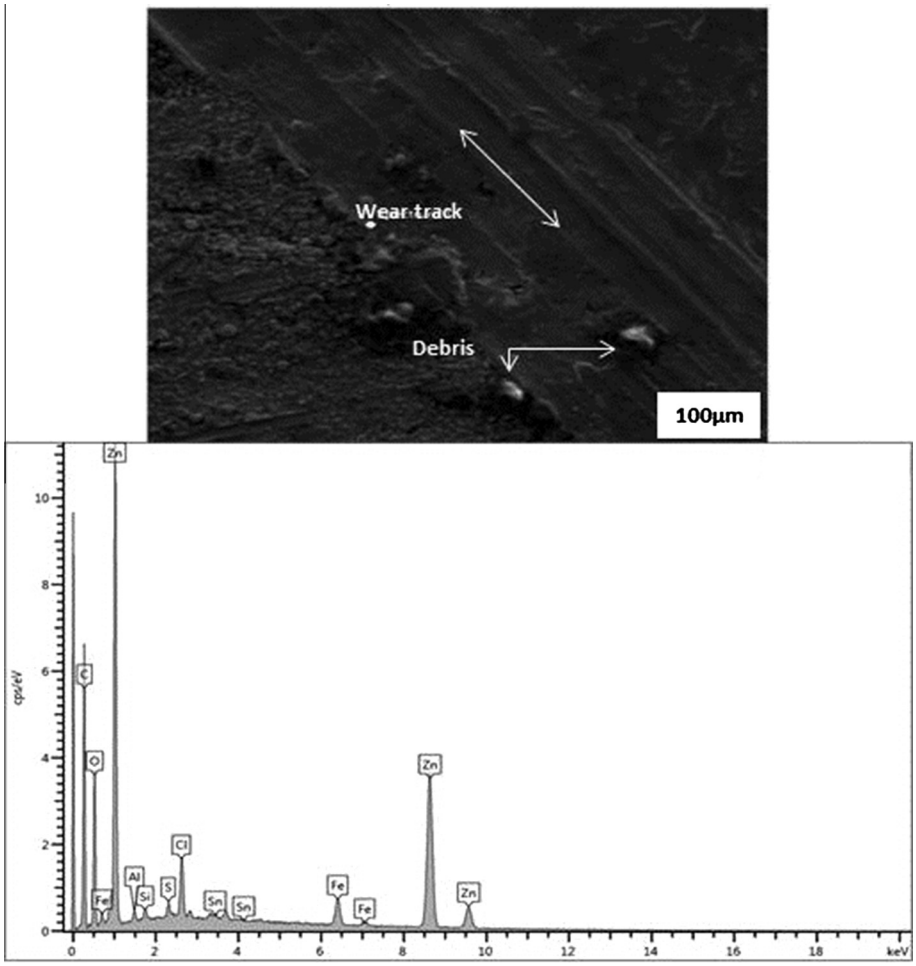

Fig. 12. SEM/EDS image of the wear scar of deposited alloy.

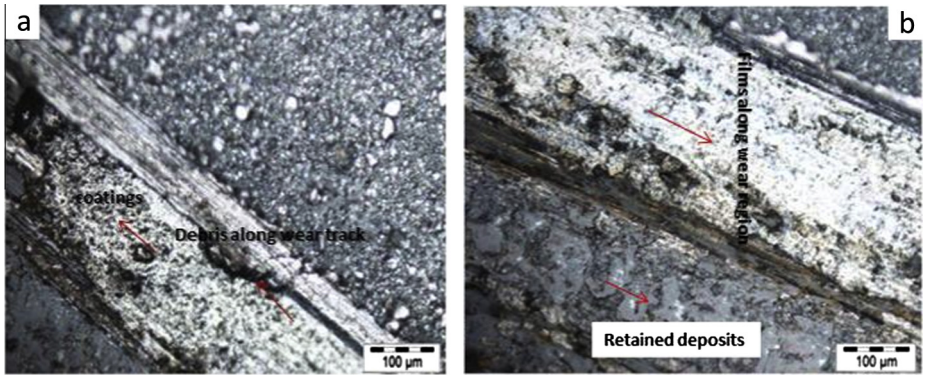

Fig. 13. OPM Micrograph of the wear scar for (a) Zn–Al–7Sn–Ti–0.3V and (b) Zn–Al–7Sn–Ti–0.3V chloride deposited sample.

more than double those of the deposited samples. The coating performance of all deposited alloy was high. Zn–Al–7Sn–Ti–0.3V produced the best performance ever among the series with display higher potential and low corrosion rate. The summarized result of polarization measurements were also illustrated in Table 3 which are obtained from Tafel plots.

The as-received sample had a polarization resistance of 2.7600 (Ω) and a high corrosion rate of about 4.1 mm/y which is expected due to lack of any surface protection as well as the exposure to chloride ion medium.

Refs. [16,22] attributed the degradation to the high anodic potential reached by the sample, absorption of the halide ion on the oxide film which took place at the oxide solution interface and the formation of basic corrosion product oxide. The corrosion current density i_{corr} of 2.71×10^{-6} A/cm^2 was obtained for Zn–Al–7Sn–Ti–0.3V alloy. This is a three order magnitude decrease as compare to the control sample. From the polarization resistance (R_p) result, the deposited alloy had 1207.7 (Ω) corrosion resistances; obviously it was the highest obtained from all the coated samples. The order of corrosion resistance is 1 > 2 > 3 > 4. The

Table 3
Summary of the potentiodynamic polarization results.

Sample No.	I_{corr} (A/cm^2)	R_p (Ω)	E_{corr} (V)	Corrosion rate (mm/y)
As-received	7.04E−02	2.7600	−1.53900	4.1
Zn–Al–7Sn–Ti–0.3V–Cl	2.19E−06	1207.7	−1.05042	0.002509
Zn–Al–7Sn–Ti–0.5V–Cl	7.68E−06	1026.1	−1.10443	0.003198
Zn–Al–13Sn–Ti–0.3V–Cl	1.58E−05	758.43	−1.20178	0.003544
Zn–Al–13Sn–Ti–0.5V–Cl	5.37E−05	269.55	−1.20239	0.005636

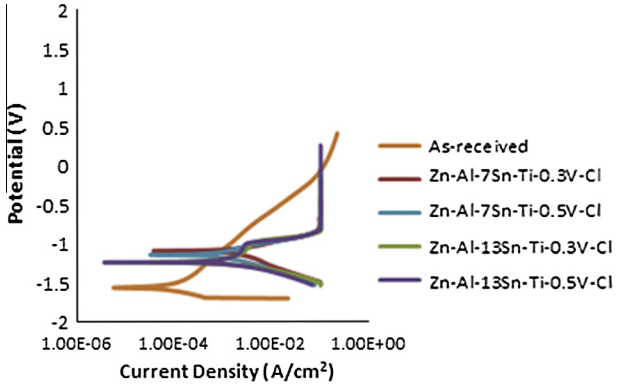

Fig. 14. Linear polarization curves for chloride deposited alloy.

electro-oxidation stability of the deposited sample are traceable to the existence of the active electronegative phases and the strong independent based active potential of the composite induced which led to strengthening characteristics.

The structural observation of the corrosion characteristics trend are seen for produce Zn–Al–7Sn–Ti–0.3V–Cl alloy using OPM after corrosion test in 3.65% NaCl solution as illustrated in Fig. 15. It is noteworthy to mention that the film scales seen are obviously in line with the report by [2] that during anodic dissolution, zinc-rich based formed excessive corrosion oxide scale and hence pose metal matrix particulate at the surfaces. The penetration of ionic halide was obviously not potent and sufficient to accelerate dissolution of the composite alloy through the coating boundaries and layer.

This progression implies that there was refusal in the chemical inertia as a result of incorporation of the alpha phase aluminum particle with the help of conjugal interference of Ti^{2+}, Sn^{2+}.

3.7. Thermal stability and micro-crystallization studies

Fig. 16 shows the thermally heat-treated hardness plot of the composite matrix at selected optimal condition. The coatings were thermo-mechanically subjected at 200 °C, 400 °C and 600 °C in an attempt to validate its stability against thermal shock at 2 h. All composite deposited samples show good degree of stability. However, with consideration of Zn–Al–7Sn–Ti–Cl–0.3V which is the best among the fabricated coated sample, it was indicated that at 400 °C in 2 h few degradation were noticed, the scales were not obvious. It will be recalled that after deposition the hardness properties of the steel move geometrically from 33.5 HVN to 298.5 HVN but the heat-treated sample have little depreciated value of 277 HVN.

This out-rightly indicates that the composite coated alloy will perform excellently well in super-heated condition over a wide range of time. Since the stability of the material is essential to validate the behavior of the coating [1,17], particles in micron could resist thermal break that might occur at the interface which may further results into crystallite build-up that promote improvement of micro hardness. At higher temperature of 600 °C appreciable

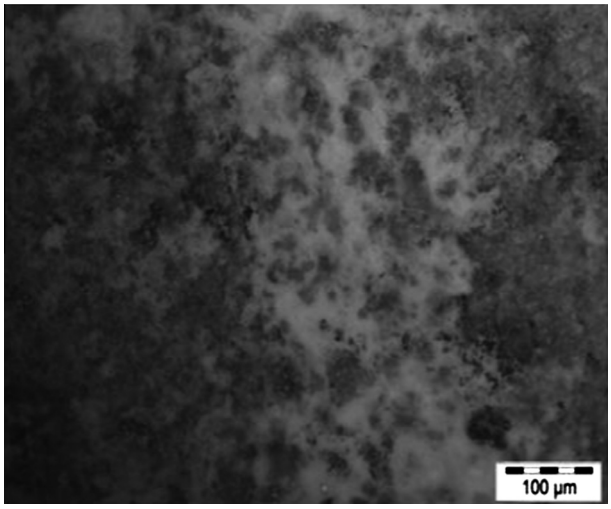

Fig. 15. OPM morphology for corroded Zn–Al–7Sn–0.3V deposited alloy.

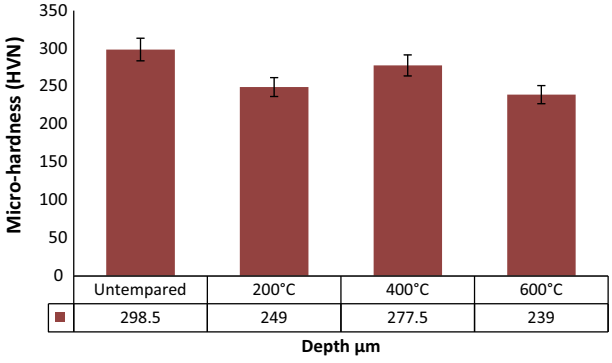

Fig. 16. Micro-hardness variation of coated and heat treated sample.

hardness result were still obtained; the real effect of isothermally heat-treated processing were observed; in practice when materials are isothermally austempered in direct atmosphere, it tend to improved hardness or possess strengthening characteristics. The life span of Zn–Al–7Sn–Ti–Cl–0.3V after thermo-mechanically treated was noticed to possess such behavior beyond expectation since stability were still retained for almost 80% from the initial coating fraction.

Fig. 17a and b presents the SEM/EDS of the thermo heated scar of the Zn–Al–7Sn–Ti–Cl–0.3V after heat-treatment in 400 °C and 600 °C for 2 h to ascertain their interfacial recrystallization tendency. It was seen that within 200–400 °C recrystallization took place and a new phase with modified orientation by amorphous structure due to the generation of Zn_7Al_2TiSn phase was observed. This is due to thermo-oxidation during slow cooling. With 600 °C a complete transformation were observed with surface brittleness at the interface. Although there were dislocations, but the plastic deformation were not so severe with evidenced by the EDS spectra shown.

The microstructure obtained show semi-coherent precipitates after 600 °C which could be attributed to slight reduction in the micro-hardness value obtain. These believe is confirmed by the report made by [22]. Interestingly SnO_2/TiO_2 particle contribute maximally to the change in the crystal and the thermal response of the fabricated coatings. The deformation resistances with little scuff observed at 600 °C were traceable to the bonding effect of the incorporated particulates.

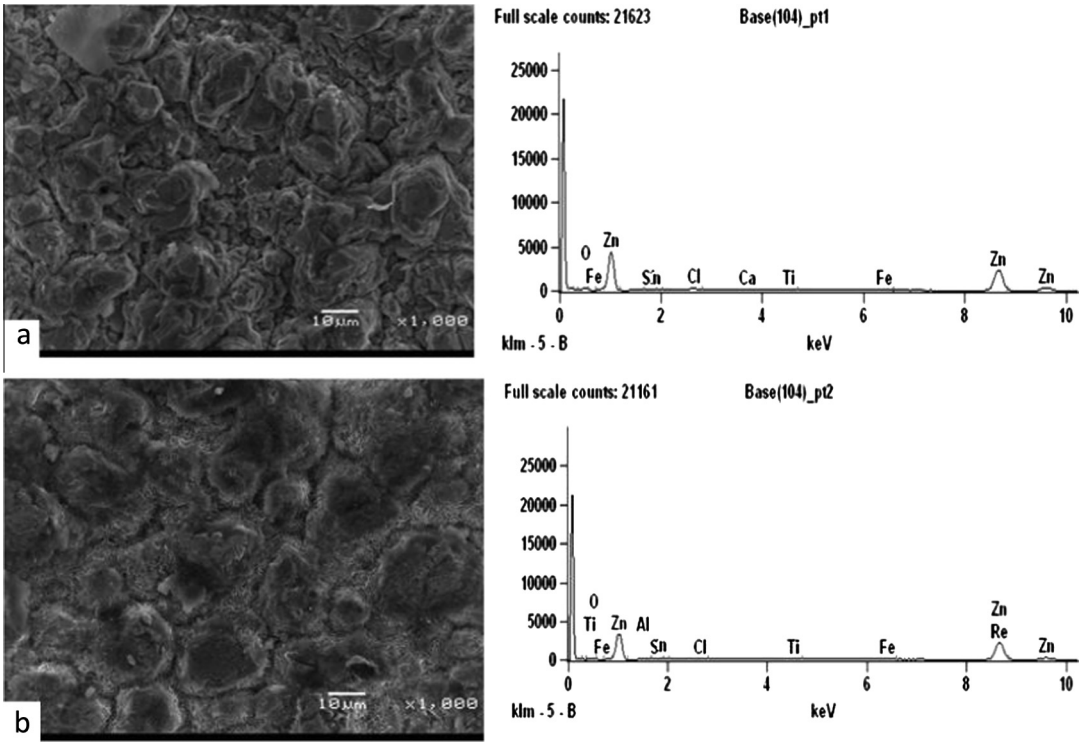

Fig. 17. SEM/EDS micrographs of heat-treated sample of Zn–Al–7Sn–Ti–Cl–0.3V at (a) 400 °C and (b) 600 °C.

Table 4
Summary of the linear polarization results of tempered Zn–Al–Sn–Ti alloy.

Sample No.	I_{corr} (A/cm^2)	R_P (Ω)	E_{corr} (V)	Corrosion rate (mm/y)
As-received	7.04E−02	2.7600	−1.53900	4.1
Zn–Al–7Sn–Ti–0.3V–Cl	2.19E−06	470.26	−1.05042	0.009134
Zn–Al–7Sn–Ti–0.3V–Cl at 600 °C	6.98E−05	83.188	−1.1481	0.810800
Zn–Al–7Sn–Ti–0.3V–Cl at 400 °C	7.39E−05	53.666	−1.1861	0.858550
Zn–Al–7Sn–Ti–0.3V–Cl at 200 °C	8.36E−05	80.331	−1.3597	0.970990

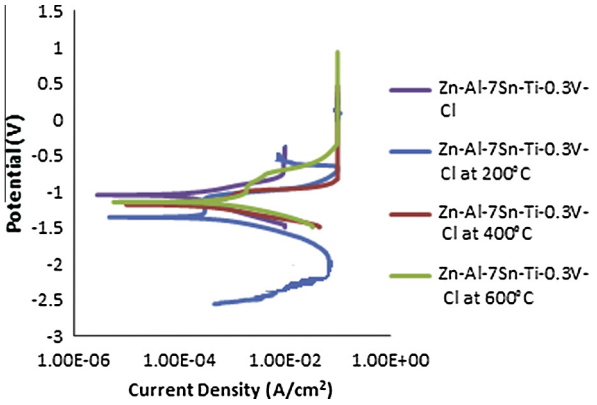

Fig. 18. Linear polarization curve of tempered Zn–Al–Sn–Ti alloy.

3.8. Electrochemical stability behavior and interfacial reaction

Fig. 18 shows the linear potentiodynamic plot of the Zn–Al–7Sn–Ti–Cl–0.3V matrix after heat-treatment in 200 °C, 400 °C and 600 °C for 2 h and compared with un-heat treated to affirm their levels of electro-oxidation and degradation behavior. The polarization data obtained from Tafel extrapolation were described in Table 4. The corrosion resistances were however favored the composites alloy coating without heat-treatment; an indication of significant correlation with the hardness stability phenomena. The trends of improvement against as-received sample also favor the heat treated composite coating in all ramification. It is a well-known fact, that chemical induced on metal in either chloride or acidic medium could enforce deterioration; secondly, stress initiation could occur when materials are subjected to thermal shock leading to drastic humiliation.

In view of this, one could observed vividly a significant resistance of the composite coated alloy even after subjected to 600 °C heat-treated processing and later checkmate its electrochemical stability. The superior properties of Sn and Ti composite on Zn rich could be attested to support the structural and thermal resistances. Al^{2+} contribution had been notice to help in the corrosion resistance of the conditioned bath leading to adhered precipitation thereby forming solid oxide thin film layer. The corrosion potential of the least corrosion observed heat-treated alloy is −1.3597 mV for Zn–Al–7Sn–Ti–0.3V–Cl at 200 °C. The best polarized is with Zn–Al–7Sn–Ti–0.3V–Cl at 600 °C with E_{corr} of −1.1481 mV. This shows an outstanding performance against the control sample with E_{corr} value of −1.53900.

The corrosion rate CR of the control sample is 4.1 mm/y. This is higher than those for the deposited and heat-treated alloy. The CR value for the deposited composite coating is 0.009134 mm/y, for the best heat treated sample is 0.810800 mm/y. Although, anticorrosion resistance properties of any composite are always seen toward modify morphology and good adhesion properties [19,26] which had been identify to be the reason for this improved property. The polarization resistance of the entire coated sample improved with the R_p values of 470.26 Ω, of the deposited alloy

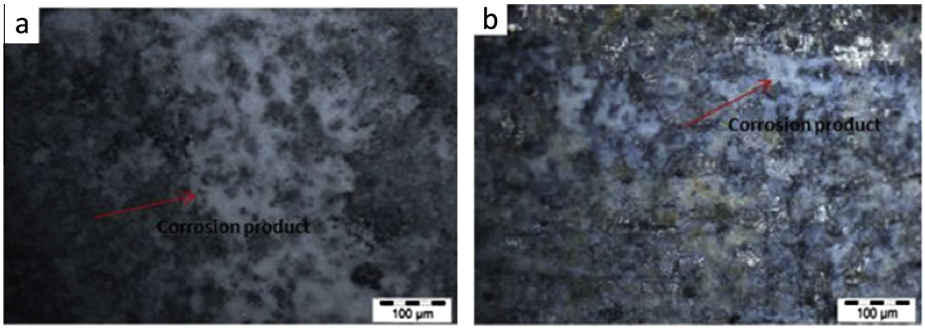

Fig. 19. Optical micrograph of the heat-treated Zn–Al–7Sn–Ti chloride deposited sample after corrosion of (a) 400 °C and (b) 600 °C.

as against the as-received substrate of 2.7600 Ω, the heat treated composite coated alloy polarized with 83.188 Ω.

Fig. 19a and b shows morphologies of Zn–Al–7Sn–Ti–S–0.3V thin film at various conditions after thermo-corrosion properties. The structure of the deposits in Fig. 19a shows the presence of initiated oxide films at the interface. The even dispersion of the crystals was not well noticed due to the impact of thermo-corrosion strain induced. From the above figure, with 600 °C corrosion process there are visible appearances of corrosion products at the coating boundaries due to initiation of thermal-oxidation activities. Obviously the presence of ions of Ti^{2+}, Sn^{2+} and most especially Al^{3+} which had a tendency of possessing oxide film, in the presence of anodic phase $Zn{\cdot}Sn_2O_3$, $TiO_7{\cdot}Sn_2O_3$ and $Al_2O_3{\cdot}Zn_3O_{12}$ could possibly generated into hydrolysis and once this occur, corrosion reaction proceed [7,25]. Moreso, Cl^- adsorbed on the oxide film sites may also alter initiation of corrosion product. Possible metallurgical reaction on oxide of Al shown below could occur as a result of the hydrolysis process.

$$Al \rightarrow Al^{3+} + 3e^- \quad (1)$$

Oxygen reduction at the cathodic reaction:

$$H_2O + 1/2(O_2) + 2e \rightarrow 2OH^- \quad (2)$$

Hence, Eqs. (1) and (2) lead to Eq. (3) with formation of metal hydroxides:

$$Al^{3+} + 3OH^- \rightarrow Al(OH)^3 \quad (3)$$

$$Al^{3+} + 3H_2O + 3Cl^- \rightarrow 3H + Al(OH)_3 + 3Cl^- \quad (4)$$

Sn^{2+}, Ti^{2+} are seen as in independent alloy variable; hence, alloy formation conditioned with Zn-rich may proceed with oxidation process

$$Zn^{2+} + 2(OH^-) \rightarrow Zn(OH)_2 \quad (5)$$

The Zn^{2+} and Al^{3+} ions in the presence Sn^{2+} and Ti^{2+} formed after oxidation of Zn ($Al \rightarrow Al^{3+}$, $Zn \rightarrow Zn^{2+}$, $Sn \rightarrow Sn^{2+}$ $Ti \rightarrow Ti^{2+}$) while OH^- releases after oxygen reduction:

$$2H_2O + O_2 + 4e^- \rightarrow 4OH \quad (6)$$

In all the repositioning of the crystal was seen and little pile up was observed. The bond after corrosion test of the heat-treated alloy slightly depreciated, although such is expected because passive film could have been disrupted by exposure of heat and aggressive chloride ions, which often cause localized corrosion observed in Fig. 19.

4. Conclusions

1. Zn–Al–Sn–Ti chloride alloy composite coatings on mild steel substrate was successfully prepared by electrolytic deposition using a zinc bath with homogeneously dispersed Al, TiO_2 and SnO_2 particles from a chloride system. Zn^{2+} and Al^{3+} in the presence of TiO_2 and SnO_2 give a significant orientation on the metal matrix.
2. For Zn–Al–7Sn–Ti–S–0.3V composite coating, it was observed from the SEM studies that the composite particles have a great influence on the deposit morphology which occurs as a result of interfacial mechanism to reduce the sizes of the particles grains.
3. Significant thermal and electrochemical stability was attained for Zn–Al–7Sn–Ti–S–0.3V coating in 3.65% NaCl. The result also shows that Ti and Sn can further increase the oxidation resistance through thermal and modified proper bath composite composition.
4. The decrease in the scale of the thin film after heat-treatment and electrochemical oxidation of the Zn–Al–7Sn–Ti–S–0.3V is essentially correlated with the effort of TiO_2 and SnO_2 effect. In general, composite coating attained higher hardness behavior, better thermo-mechanical stability and improved wear resistance due to the inclusion of the composite particle.
5. The wear friction coefficient was improved geometrically as against the as-received sample.

Acknowledgements

This material is based upon work supported financially by the National Research Foundation South Africa. The equipment support by Surface Engineering Research Centre (SERC) Tshwane University of Technology, Pretoria is deeply appreciated.

References

[1] O.S.I. Fayomi, A.P.I. Popoola, V.S. Aigbodion, J. Alloys Comp. 617 (2014) 455.
[2] B.M. Praveen, T.V. Venkatesha, Appl. Surf. Sci. 254 (2008) 2418.
[3] L. Chuen-Chang, H. Chi-Ming, J. Coat. Technol. Res. 3 (2006) 99.
[4] O.S.I. Fayomi, A.P.I. Popool, Int. J. Electrochem. Sci. 8 (2013) 11502.
[5] S. Hongmark, P. Hedenqvist, S. Jacobson, J. Surf. Coat. Technol. 90 (1997) 247.
[6] K.H. Zum Gahr, Wear 200 (1996) 215.
[7] A.A. Volinsky, J. Vella, I.S. Adhihetty, V.L. Sarihan, L. Mercado, B.H. Yeung, W.W. Gerberich, Mat. Res. Soc. 649 (2001) 6.
[8] R.E. Melchers, J. Corros. Sci. 49 (2007) 3149.
[9] A.P.I. Popoola, O.S. Fayomi, Int. J. Electrochem. Sci. 6 (2011) 3254.
[10] M.M. Abou-Krisha, F.H. Assaf, S.A. El-Naby, J. Res. Coat. Technol. 6 (2009) 391.
[11] M.J. Rahman, S.R. Sen, M. Moniruzzaman, K.M. Shorowordi, J. Mech. Eng. 40 (2009) 9.
[12] M. Arici, H. Nazir, A. Aksu, J. Alloys Comp. 509 (2011) 1534.
[13] R. Xu, J. Wang, Z. Guo, H. Wang, J. Rare Earth 26 (2008) 579.
[14] G. Yang, S. Chai, X. Xiong, S. Zhang, L. Yu, P. Zhang, Trans. Nonferr. Met. Soc. China 22 (2012) 366.
[15] O. Sancakoglu, O. Culha, M. Toparli, B. Agaday, E. Celik, J. Mater. Des. 32 (2011) 4054.
[16] T.G. Wang, D. Jeong, Y. Liu, S. Lyengar, S. Melin, K.H. Kim, J. Surf. Coat. Technol. 206 (2012) 2638.
[17] O. Hammami, L. Dhouibi, P. Bercot, E.M. Rezrazi, E. Triki, Int. J. Corros. Sci. 8 (2012) 1.
[18] O.S.I. Fayomi, M. Abdulwahab, A.P.I. Popoola, J. Ovonic Res. 9 (2013) 123.

[19] W. Zhang, W. Liu, C. Wang, J. Eur. Ceram. Soc. 22 (2002) 2869.
[20] J. Fustes, A.D.A. Gomes, M.I. Silva Pereira, J. Solid State Electrochem. 121 (2008) 1435.
[21] D. Dong, X.H. Chen, W.T. Xiao, G.B. Yang, P.Y. Zhang, Appl. Surf. Sci. 255 (2009) 7051.
[22] A.P.I. Popoola, O.S.I. Fayomi, O.M. Popoola, Int. J. Electrochem. Sci. 7 (2012) 4898.
[23] H. Kazimierezak, P. Ozga, Surf. Sci. 607 (2013) 33.
[24] J.L. Mo, M.H. Zhu, B. Lei, Y.X. Leng, N. Huang, Depos. Phys. Vap. Depos. Wear 263 (2007) 1423.
[25] B. Subramanian, S. Mohan, S. Jayakrishnan, Surf. Coat. Technol. 201 (2006) 1145.
[26] O.S.I. Fayomi, A.P.I. Popoola, Res. Chem. Intermed. Res. 39 (2013) N06. <http://dx.doi.org/10.1007/s11164-013-1354-2> ISSN 0922-6168.
[27] A.P.I. Popoola, O.S.I. Fayomi, O.M. Popoola, Int. J. Electrochem. Sci. 7 (2012) 4860.
[28] X. Xuli, Z. Igor, R.M. Joseph, J. Mat. Sci. Technol. 209 (2009) 2632.
[29] K. Vathsala, T.V. Venkatesha, J. Appl. Surf. Sci. 257 (2011) 8929.
[30] D. Blejan, L.M. Muresan, Mat. Corros. 63 (2012) 1.